Geotech Geol Eng
https://doi.org/10.1007/s10706-023-02716-x

ORIGINAL PAPER

Prediction of Soil–Water Characteristic Curves in Bimodal Tropical Soils Using Artificial Neural Networks

Sávio Aparecido dos Santos Pereira · Arlam Carneiro Silva Junior · Thiago Augusto Mendes · Gilson de Farias Neves Gitirana Junior · Roberto Dutra Alves

Received: 20 July 2023 / Accepted: 27 November 2023

Abstract Laborious and time-consuming tests are required for the determination of the soil–water characteristic curve (SWCC), often leading to the adoption of estimation methods. To answer the challenge of SWCC prediction, numerous pedotransfer functions (PTF) have been developed. Yet, previous studies have not considered the special behavior of bimodal tropical soils. These materials present dual porosity that is generally attributed to particle aggregation. This paper presents a novel PTF, specifically designed for bimodal tropical soils and based on artificial neural networks (ANNs). The model was trained and tested utilizing a database that was assembled containing soils from tropical regions of Brazil and featuring data for the grain-size distribution (GSD), consistency limits, and SWCC. Natural and remolded soils were included in the training database, but no distinction between soil conditions was made in the ANN. GSDs in the aggregated and disaggregated states were used to offer information to the ANN regarding the effect of particle aggregation on the water retention. The developed model was able to reproduce the typical SWCC shape of bimodal soils. Predictions for the degree of saturation were moderately correlated with directly measured data, with a coefficient of determination of 0.69. The air-entry value and residual suction of the macropores proved to be the most difficult SWCC attributes to be estimated. The ANN presented superior performance when compared to other PTFs not designed specifically for bimodal tropical soils, such as the Arya-Paris and ROSETTA models. It can be concluded from the obtained results that the developed ANN architecture

Supplementary Information The online version contains supplementary material available at https://doi.org/10.1007/s10706-023-02716-x.

S. A. dos Santos Pereira (✉) · A. C. Silva Junior
Federal Institute of Education, Science and Technology of Goiás, Aparecida de Goiânia 74968-755, Brazil
e-mail: savioaparecido1@gmail.com

A. C. Silva Junior
e-mail: arlam.junior@ifg.edu.br

Present Address:
S. A. dos Santos Pereira · G. d. Gitirana Junior · R. D. Alves
School of Civil and Environmental Engineering, Universidade Federal de Goiás (UFG), Goiânia 74605-220, Brazil
e-mail: gilsongitirana@ufg.br

R. D. Alves
e-mail: roberto.dutra@hotmail.com

T. A. Mendes
Graduate Program in Technology, Management and Sustainability (in Portuguese: Programa de Pós-Graduação em Tecnologia, Gestão e Sustentabilidade, PPGTGS), Federal Institute of Education, Science and Technology of Goiás, Goiânia 74055-110, Brazil
e-mail: thiago.mendes@ifg.edu.br

Published online: 27 December 2023

and general approach showed a high capability to capture the main features of the SWCC.

Keywords Water retention · Lateritic soils · Tropical soils · Unsaturated soils · Machine learning

1 Introduction

The study of soils under unsaturated conditions involves modeling infiltration, evaporation, diffusion, and volume change, among other processes. In this context, the soil–water characteristic curve (SWCC) plays a central role, giving the relationship between water content and water potential. The SWCC is also essential for estimating other properties of unsaturated soils (Fredlund 2000; Zhai et al. 2020), such as the permeability function (Fredlund et al. 1994; Amadi et al. 2023) and the shear strength envelope (Vanapalli et al. 1996; Fredlund et al. 1996; Pham et al. 2023).

Unfortunately, the field and laboratory tests available for determining the SWCC are laborious and time-consuming. To make the determination of the SWCC practical in situation where large volumes of data are involved and in preliminary studies, pedotransfer functions (PTFs) have been developed. These PTFs use physical properties of the soil that are easier and less expensive to obtain. The main input physical property used by PTFs is the grain-size distribution (GSD), but several other properties have been utilized such as the Atterberg limits and bulk density. The GSD has been used by several authors to estimate the pore-size distribution (Arya and Paris 1981; Alves et al. 2020; Silva et al. 2020; Campos-Guereta et al. 2021; Satyanaga et al. 2023; Zhai et al. 2023).

In general, the great majority of PTFs are developed for soils of temperate climate regions. For tropical soils, the modeling of the SWCC becomes particularly challenging given their complex pore structure (Sobotkova et al. 2011; Miguel and Bonder 2012; Araujo et al. 2017; Camapum de Carvalho and Gitirana Jr. 2021; Foko Tamba et al. 2022; Falcão et al. 2023). Tropical soils often present macro and micropores (in some cases mesopores can also be found), resulting in bimodal or multimodal pore-size distributions (PSDs). Bimodal PSDs result from particle aggregations, which can be identified by comparing the GSD with and without disaggregation (Miguel and Bonder 2012; Camapum de Carvalho and Gitirana Jr. 2021; Falcão et al. 2023). A bimodal PSD produces an SWCC with two or three desaturation stages, each corresponding to a pore family (Araujo et al. 2017; Camapum de Carvalho and Gitirana Jr. 2021).

Some studies have been published on the development of PTFs for tropical soils, such as Tomasella and Hodnett (1998), Tomasella et al. (2000) and Ottoni et al. (2018). However, only unimodal tropical soils have been considered in these previous studies. The limited number of investigations of PTFs for tropical soils, especially for bimodal soils, and the singularities in terms of their structure and behavior, makes the development of a PTF for such soils particularly urgent.

Machine learning techniques arise as alternative methods to overcome the great complexity of the physical properties of tropical soils and their relationships with the SWCC. The main approach used was Artificial Neural Networks (ANN), which were adopted by Melo and Pedrollo (2015), D'Emilio et al. (2018), Li and Vanapalli (2021), and others. However, once again, only few PTFs utilizing ANN have been developed for tropical soils (Minasny et al. 1999; Minasny and McBratney 2002; Albuquerque et al. 2022) and none for bimodal tropical soils have been found.

In this context, this paper presents a novel PTF, specifically designed for the prediction of the SWCC of tropical bimodal soils. The PTF is based on the GSD with and without particle disaggregation, liquid limit (w_L), and plastic index (PI) and should offer a framework that can be improved in the future as more data becomes available.

2 Background on the Use of Artificial Neural Networks for the Prediction of the SWCC

ANNs consist of a machine learning approach that seeks to establish a relationship between input and output parameters based on biological concepts and principles of the human neural network (Minasny and McBratney 2002; Jain et al. 2004; Souza et al. 2022). Since the 90s, several authors have developed SWCC prediction models using ANNs, such as Schaap et al. (2001), Minasny and McBratney (2002),

Haghverdi et al. (2012), and Rudiyanto et al. (2021). Figure 1 shows a typical setup of an ANN employed for the prediction of the SWCC and Table 1 summarizes the main features of ANNs designed for SWCC prediction.

The main ANN model used for this type of application, as shown in Fig. 1, is the multilayer Perceptron (Pachepsky et al. 1996; Minasny and McBratney 2002; Pham et al. 2019). This type of ANN is composed of an input layer, an output layer, and intermediate layers called hidden layers. Each element in an intermediate layer is called a neuron. Neurons represent the linear product between weights and the values of the previous layer (Melo and Pedrollo 2015; Rudiyanto et al. 2021). The weights are optimized during the training stage.

Table 1 indicates that, in general, ANNs developed for SWCC prediction have used an intermediate layer with a number of neurons ranging from 1 to 138 (Belik et al. 2019; Haghverdi et al. 2018). The number of intermediate layers is also variable, between 1 and 10. Care must be taken when choosing the number of neurons in the layer and the number of intermediate layers because it may increase the difficulty in optimizing the network and cause overfitting or underfitting (Minasny and McBratney 2002; Pham et al. 2019). Overfitting is the loss of predictive capability of the ANN for data outside the training base. Underfitting is the lack of predictive ability of the ANN even within the range of training information.

Neurons are enabled by an activation function (Haykin 1999; Minasny and McBratney 2002). The activation functions give a non-linear character to ANNs. This function is used in intermediate and output layers. The main activation functions used in ANNs for prediction SWCC are the hyperbolic tangent, the sigmoid function, and the linear function, as shown in Table 1.

The optimization of the ANN is done using the backpropagation algorithm (Fig. 1). During backpropagation, initial values are calculated for the network and the weights are fitted until the optimal ANN is obtained. The definition of the optimal network is given by an error metric. In SWCC prediction, the following metrics are often used for error evaluation: the root mean squared error (RMSE), the mean square error (MSE), and the mean absolute error (MAE) (Minasny and McBratney 2002; Haghverdi et al. 2018; Amanabadi et al. 2019). As for the algorithm used to minimize the error, the stochastic gradient descent stands out, but there are other algorithms, such as Adam and RMSProp (Haykin et al. 1999).

The amount of data available to be used for ANN training and testing is important in the establishment of its range and generalization capacity. Table 1 indicates that previous SWCC prediction models using ANN used databases with 135–7094 data points. The percentage of data points used for training ANNs for SWCC estimation varied between 56 and 100%. Only Jain et al. (2004) used 100% of data for training, making it impossible to independently evaluate the model performance. The number of epochs is also important, to avoid overfitting or underfitting (Melo and Pedrollo 2015; Pham et al. 2019). The number of epochs used in ANNs for SWCC prediction has ranged from 50 to 50,000.

ANNs for SWCC prediction have been developed using various input parameters and multiple parameterization options for the network output, as shown in

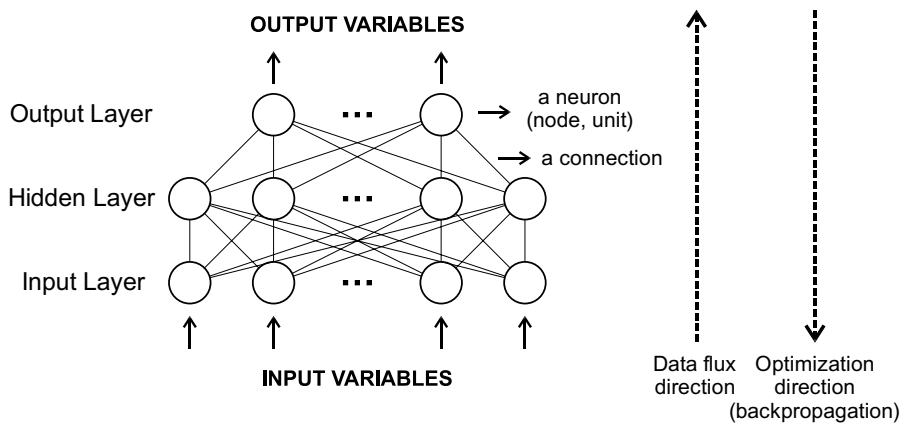

Fig. 1 Typical ANN arrangement used in SWCC prediction [modified from Pachepsky et al. (1996)]

Table 1 Summary of the main characteristics of ANN models for the prediction of the SWCC

Output	Input*	Number of hidden layers	Number of neurons in the hidden layer	Activation functions used in the hidden layer	Activation functions used in the output layer	Number of epochs	Database size	Training base (%)	R^2
Coefficients of the fitting equation	Soil texture, GSD, bulk density, porosity and plasticity limits	1–10	1–138	hyperbolic tangent and sigmoid	hyperbolic tangent, sigmoid, and linear function	60–50.000	147–7094	56–100	0.65–0.99
Water content values for given suction values	Soil texture, GSD, bulk density, and porosity	1–5	3–30	hyperbolic tangent, and sigmoid	hyperbolic tangent, sigmoid, and linear function	50–20.000	148–894	64–100	0.60–0.95
Water content values with suction value as input parameter	Soil texture, bulk density, organic matter presence and matric potential	1–5	1–54	hyperbolic tangent, RELU function, and sigmoid	sigmoid and linear function	50–20.000	135–2187	64–90	0.32–0.99

Sources: Pachepsky et al. (1996), Schaap and Bouten (1996), Schaap and Leij (1998), Koekkoek and Bookltink (1999), Minasny et al. (1999), Schaap et al. (2001), Minasny and McBratney (2002), Jain et al. (2004), Skalová et al. (2011), Haghverdi et al. (2012), Bayat et al. (2013), Melo and Pedrollo (2015), D'Emilio et al. (2018), Haghverdi et al. (2018), Saha et al. (2018), Achieng (2019), Bayat et al. (2019), Belik et al. (2019), Pham et al. (2019), Javanshir et al. (2020), Li and Vanapalli (2021), Rudiyanto et al. (2021), Xu et al. (2021), Garg et al. (2022), and Rastgou et al. (2022)

*Only the main inputs parameters are listed

Table 1. Data from the GSD are widely used as input, either in terms of the soil textural percentages or the grain diameter for a certain percentage passing values. Indirectly obtained parameters have also been utilized, such as the PSD parameters. The GSD has been often adopted since it provides indirect information regarding the PSD (Sillers et al. 2001; Silva et al. 2008). It should be noted that other parameters are also often incorporated as input values, such as bulk density, consistency limits, organic matter content.

There is no consensus regarding the ideal SWCC parametrization alternative used in the development of ANNs. Three options are commonly adopted: water content for predefined suction values, water content for user-specified suction values, and the coefficients of a fitting equation. Determining water content from user-defined suction was called a pseudo-continuous approach by Haghverdi et al. (2012).

In general, SWCC prediction models using ANN are aimed at soils from temperate climate regions with unimodal behavior. However, Minasny and McBratney (1999) developed a PTF using ANN for the soils of Australia that can be considered tropical soils. The ANN estimates the parameters of the van Genuchten equation, therefore being restricted to unimodal behavior. Minasny and McBratney (1999) presented two approaches to predict the coefficients of the van Genuchten (1980) equation: obtaining the coefficients of the fitting equation directly from ANN (neuro-p); readjust the weights of the ANN, performing a second fit of the ANN minimizing the difference between the predicted points of SWCC and the respective experimental points (neuro-m). The neuro-m method gave better performance compared to the neuro-p method.

Finally, regarding the performance of the ANNs developed in general, R^2 values ranging from 0.32 to 0.99 were obtained, as show in Table 1. This demonstrates the predictive capabilities of ANNs for SWCCs. The Flexible nature of ANNs indicates that is may be a promising approach for the prediction of the SWCC of complex bimodal soils.

3 Materials and Methods

3.1 Collection and Processing of Soil Data

Data records of soils including the SWCC, GSD, w_L and PI were obtained in papers, dissertations, and thesis published between 2008 and 2020 that presented experimental research programs on bimodal tropical soils. Documents that did not present one or more of the four study variables (i.e., SWCC, GSD, w_L, and PI) were discarded. Only papers that presented the GSD with and without disaggregation were collected. The requirement of two GSDs assumed that the GSDs of the soil in the aggregated and disaggregated states would provide useful microstructural information during the learning process of the ANN.

The SWCC predictions will reflect the SWCCs employed for training the neural network. All SWCCs used during the modeling exercise correspond to natural and compacted soils. No distinction was made between these two conditions when training the ANN. However, it is common knowledge that the structure/fabric of a material will change when it is compressed in-situ, disturbed and subsequently remolded, or affected by other means (Qian et al. 2022). Recognizing that porosity and saturated water content are the main variables affected by in-situ soil compression and by disturbing and remolding the soil (Ng and Pang 2000; Rahardjo et al. 2012; Zhou et al. 2012), the ANN model was developed in terms of degree of saturation.

Regarding the geographic distribution, only data on soils from the Brazilian Central-West Region were considered. The selected papers, thesis, and dissertations were the following: Silva (2009), Aguiar (2010), Araújo (2010), Matos (2011), Farias (2012), Luiz (2012), Jesus (2013), Aguiar (2014), Borges (2014), Carvalho (2014), Dias (2014), Diemer (2014), Grau (2014), Almeida et al. (2015), Gomes (2015), Queiroz (2015), Angelim et al. (2016), Lopera (2016), Ayala (2020), Freitas et al. (2020), Wanderley Neto (2020) and Mendes et al. (2022).

Experimental SWCC data points for matric and total suction were collected from the chosen publications. Total suction values were obtained only for values above 1500 kPa, as recommended by Fredlund et al. (2012). The selected SWCC data includes wetting, drying, and combined paths. All volumetric and gravimetric water content data were converted to the degree of saturation by considering the soil volume change during testing, which is typically negligible for tropical bimodal materials.

Data was collected using a variety of testing procedures, namely: pressure and suction plate, filter paper, psychrometer, and centrifuge method. Figure 2 shows

the proportions of each test in the database. The filter paper method is predominant, due to its simplicity and low cost (Leong et al. 2002). Specimens are subjected to various water contents by wetting or drying while monitoring the total weight of the soil. Therefore, it is difficult to obtain data points between the first residual suction and the second air-entry value, where small changes in water content correspond to large variations in suction. Fortunately, this type of gap in data points does not compromise the complete delineation of the SWCC.

Specific fitting equations are required for bimodal soils. Some of the available equations for bimodal SWCCs are the double van Genuchten function (Carducci et al. 2011), the discrete–continuous multimodal van Genuchten model (Yan et al. 2021), the model proposed by Zhao et al. (2023) for multimodal soils, and the bimodal equation developed by Gitirana Jr. and Fredlund (2004). The Gitirana Jr. and Fredlund (2004) model was selected herein (Eq. 1) because the coefficients of the fitting equation have physical meaning which can be easily used in other applications, as shown in Fig. 3.

$$S = \frac{S_1 - S_2}{1 + (\psi / \sqrt{\psi_{b1}\psi_{res1}})^{d1}} + \frac{S_2 - S_3}{1 + (\psi / \sqrt{\psi_{res1}\psi_{b2}})^{d2}} + \frac{S_3 - S_4}{1 + (\psi / \sqrt{\psi_{b2}\psi_{res2}})^{d3}} + S_4 \quad (1)$$

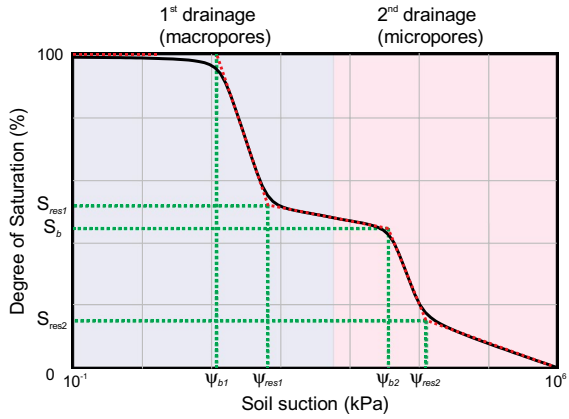

Fig. 3 Graphic representation of the input parameters of Gitirana Jr. and Fredlund (2004) equation

$$S_i = \frac{\tan\theta_i(1 + r_i^2)\ln(\psi/\psi_i^a)}{(1 - r_i^2\tan^2\theta_i)} + (-1)^i \frac{(1 + \tan^2\theta_i)}{(1 - r_i^2\tan^2\theta_i)} \sqrt{r_i^2\ln^2(\psi/\psi_i^a) + \frac{a^2(1 - r_i^2\tan^2\theta_i)}{(1 + \tan^2\theta_i)}} + S_i^a \quad (2)$$

where $i = 1, 2, 3$ e 4; $\psi_1^a = \psi_{b1}$, $\psi_2^a = \psi_{res1}$, $\psi_3^a = \psi_{b2}$, $\psi_4^a = \psi_{res2}$, $\psi_5^a = 10^6$; $S_1^a = 1$, $S_2^a = S_{res1}$, $S_3^a = S_b$, $S_4^a = S_{res2}$, $S_5^a = 0$; $\lambda_0 = 0$, $\lambda_1 = \arctan\{(S_1^a - S_{i+1}^a)/[\ln(\psi_{i+1}^a - \psi_i^a)]\}$ are the desaturation slopes; $r_i = \tan[(\lambda_{i-1} - \lambda_i)/2]$ are the aperture angle tangents; $\theta_i = -(\lambda_{i-1} + \lambda_i)/2$ are the hyperbolas' rotation angles; $j = 1$, 2, 3;

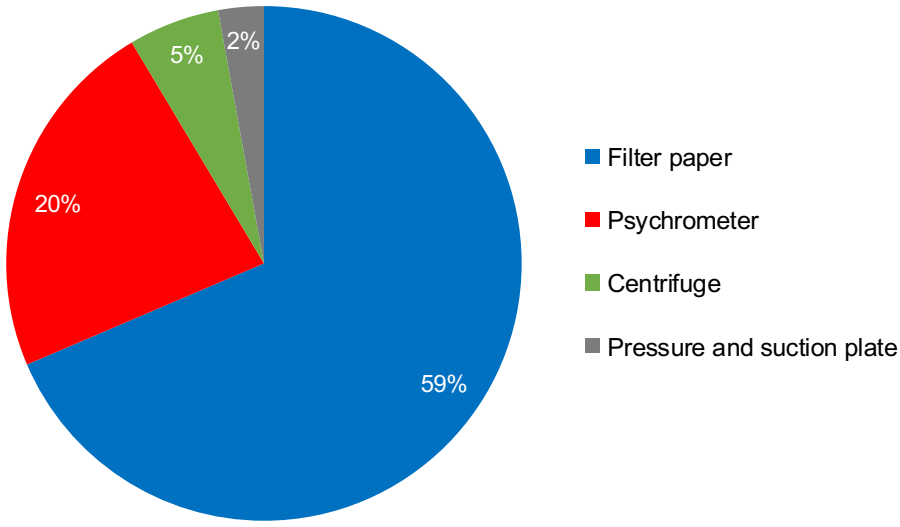

Fig. 2 Types of SWCC tests collected for the database

$d_j = 2\exp[1/\ln(\psi_{j+1}^a/\psi_j^a)]$ are weight factors; ψ_{b1} is the first air-entry value of suction (kPa); ψ_{res1} is the first residual suction (kPa); S_{res1} is the first residual degree of saturation; ψ_{b2} is the second air-entry value of suction (kPa); S_b is the air-entry value of degree of saturation; ψ_{res2} is the second residual suction (kPa); S_{res2} is the second residual degree of saturation; a is hyperbolas sharpness variable;

Figure 3 presents a graphical representation of the input parameters for the Gitirana Jr. and Fredlund (2004) equation. The equation encompasses the complete suction range, from 0 to 10^6 kPa. In fact, the complete suction range was considered during the fitting and prediction procedures. The best fit of Eq. 1 was carried out using Microsoft Excel's Solver tool. An initial guess was manually defined to ensure convergence, as recommended by Gitirana Jr. and Fredlund (2004).

A total of 55 SWCCs and 870 data points were collected from the literature. In other words, 55 records were considered for this network, which was then divided into training and test data. Table 2 presents a statistical description of the obtained best-fit SWCC parameters. The soil suction parameters (i.e., air-entry values and residual suctions) are presented in their original form and as their natural logarithm values. A significant reduction in the coefficient of variation can be seen when taking the natural logarithm values. This situation was also observed by Gitirana Jr. and Fredlund (2016). These authors performed an extensive statistical analysis and concluded, through normality tests, that suction parameters follow a log-normal distribution. The use of soil suction in logarithmic form can be found in other works that have developed ANNs for SWCC prediction, such as Jain et al. (2004). Previous findings and the information presented in Table 2 indicate that the utilizing the natural logarithms of suction can be a facilitator for ANN training.

The GSD is an important input parameter for the developed ANN. For the GSD, which in general is presented in a nonparametric manner, it was necessary to perform a parameterization to harmonize the data. The parametrization was accomplished by adopting as variables the percentages of gravel, sand, silt, and clay, as defined by the International Standardization Organization and *Comité Européen de Normalisation* (ISO/CEN) standard. Gravel corresponds to particles larger than 2 mm, sand to the particles between 0.06 and 2 mm in diameter, silt refers to particles between 0.06 and 0.002 mm in diameter and clay particles are smaller than 0.002 mm. For all soils, both GSDs with and without disaggregation were taken, simultaneously, as input to the ANN.

The liquid and plastic limits values did not need to undergo any type of treatment or parametrization. The liquid limit values of all soils were determined using the Casagrande apparatus whereas the plastic limit followed the cylinder molding technique, as standardized by ABNT NBR 6459 (2016a) and ABNT NBR 7180 (2016b), respectively. Table 3 presents a statistical summary of the data collected for

Table 2 Statistical description of the best fit SWCC parameters of the Gitirana Jr. and Fredlund (2004) equation (N = 55)

Parameters	Minimum	Maximum	Mean	Standard deviation	*COV** (%)
ψ_{b1}	0.03	81.2	6.9	14.6	213
$\ln(\psi_{b1})$	−3.5	4.4	0.6	1.6	264
ψ_{res1}	3.9	860.6	50.0	133.7	268
$\ln(\psi_{res1})$	1.4	6.8	3.0	1.0	34
S_{res1}	0.30	0.85	0.52	0.14	28
ψ_{b2}	105.3	89,571.5	8,455.8	12,007.2	142
$\ln(\psi_{b2})$	4.7	11.4	8.3	1.5	17
S_b	0.20	0.80	0.41	0.16	38
ψ_{res2}	588.2	292,131.2	27,177.39	40,290.9	149
$\ln(\psi_{res2})$	6.4	12.6	9.7	1.0	10
S_{res2}	0.01	0.25	0.05	0.06	110
a	0.02	0.08	0.05	0.03	56
SSD**	0.000	0.258	0.024	0.041	169

**COV* Coefficient of variation

***SSD* Sum of squared deviations

Table 3 Statistical description of the collected data: GSD (with and without disaggregation), liquid limit, plastic limit, and plasticity index (N = 49)

Variables	Minimum	Maximum	Mean	Standard deviation	*COV* (%)
% of gravel	0	35	2	7	232
% of sand with disaggregation	0	77	49	20	41
% of silt with disaggregation	7	64	26	14	54
% of clay with disaggregation	0	91	22	25	113
% of sand without disaggregation	31	95	61	14	24
% of silt without disaggregation	0	68	31	14	46
% of clay without disaggregation	0	37	6	11	188
Liquid limit (w_L), %	24	54	39	6	15
Plastic limit (w_P), %	0	42	25	6	25
Plastic index (PI), %	5	36	14	4	33

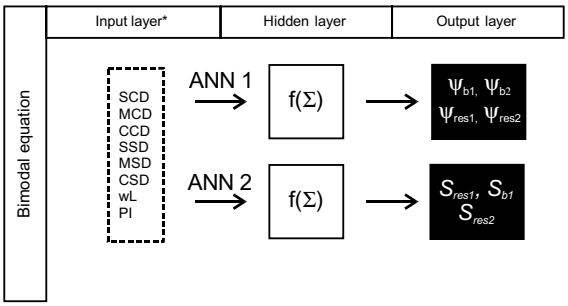

Fig. 4 Overview of implementations of ANN for SWCC prediction. **SCD* % sand, disaggregated, *MCD* % of silt, disaggregated, *CCD* % clay, disaggregated, *SSD* % sand, aggregated, *MSD* % of silt, aggregated, *CSD* % clay, aggregated, *LL* Liquid limit, *PI* Plasticity index

the GSD parameters (with and without disaggregation), w_L, w_P (plastic limit), and *PI*.

3.2 Artificial Neural Networks

The Keras library (KERAS 2022), a deep learning development API of the TensorFlow platform, was used to build the ANNs. Figure 4 shows a panorama of the ANN architecture, designed to predict the coefficients of the equation proposed by Gitirana Jr. and Fredlund (2004) including the input and output parameters of each network. The complex relationship between the SWCC and basic soil properties may prompt researchers to incorporate many input parameters, to capture more features of soil behavior. However, predictive ANN models are designed to offer approximate estimations that are not intended to fully replace soil testing. Moreover, estimation models need to be based on commonly available input data, to have practical relevance. Therefore, the selected input parameters reflect this understanding of what should be the goal of the developed ANN.

According to the classification of predictive output of Minasny and McBratney (2002), the traditional neuro-p method was chosen, without a second fitting of the weights after ANN prediction. The architecture of each ANN, that is, the number of neurons in each layer and the activation functions used, will be detailed in the presentation of results. To obtain an optimal network, several tests were performed, varying the number of layers, the number of neurons per layer, and the activation functions to be used. There is a wide range of techniques of network development, such as Bayesian hyperparameter optimization. However, traditional empiricism (trial-and-error method) was adopted, which is quite common in the study of neural networks for predicting SWCC (Jain et al. 2004; Ebrahimi et al. 2014; Melo and Pedrollo 2015; Li and Vanapalli 2021).

The coefficients of the equations studied were determined using distinct networks. This strategy was designed due to the wide difference of domain between the variables, with the degree of saturation ranging between 0 and 1 and the natural logarithm values of the soil suction parameters fluctuating between − 3.5 and 12.6 (Table 2). Both ANNs used the same training data, test data, and input parameters (Fig. 4).

The suction coefficients (i.e., ψ_{b1}, ψ_{res1}, ψ_{b2}, and ψ_{res2}) were evaluated in the natural logarithm scale, as described in the previous section. The natural logarithm values were rescaled to the interval between -1

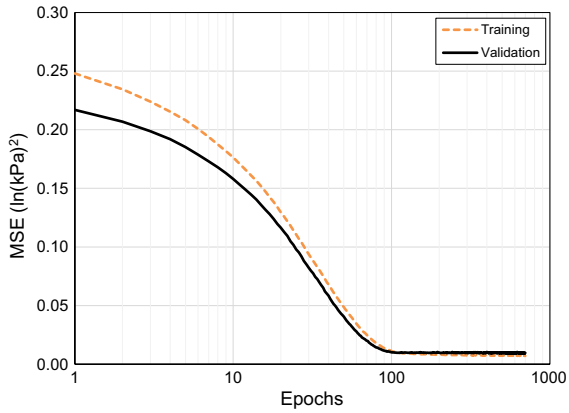

Fig. 5 MSE throughout the training and validation of the ANN 1

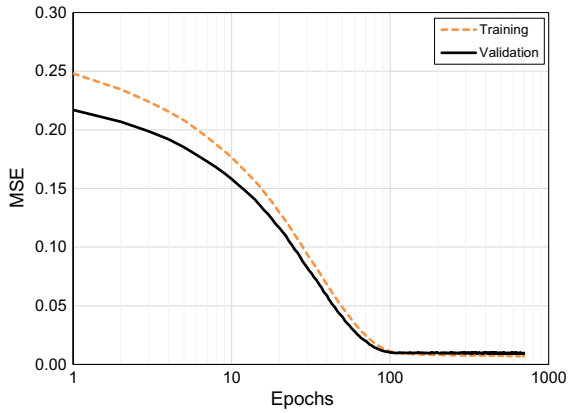

Fig. 7 *MSE* throughout the training and validation of the ANN 2

and 1, same approach adopted by Jain et al. (2004). This conditioning was performed because the output function used in the network was the hyperbolic tangent, which also presents a domain between -1 and 1. No rescaling was required for the degree of saturation parameters (i.e., S_{res1}, S_b and S_{res2}). Finally, the SWCC equation parameter a was fixed as 0.05, corresponding to the average presented in Table 2. This choice was made because a is a shape parameter of secondary importance and variations have minor impact on the overall position and shape of the SWCC.

The input parameters of the ANNs were selected based on their availability and are believed to be some of the most fundamental variables describing the physical and mineralogical characteristics of the soil. Special attention must be given to the fact that GSDs corresponding to both aggregated and disaggregated conditions are required as input parameters. The

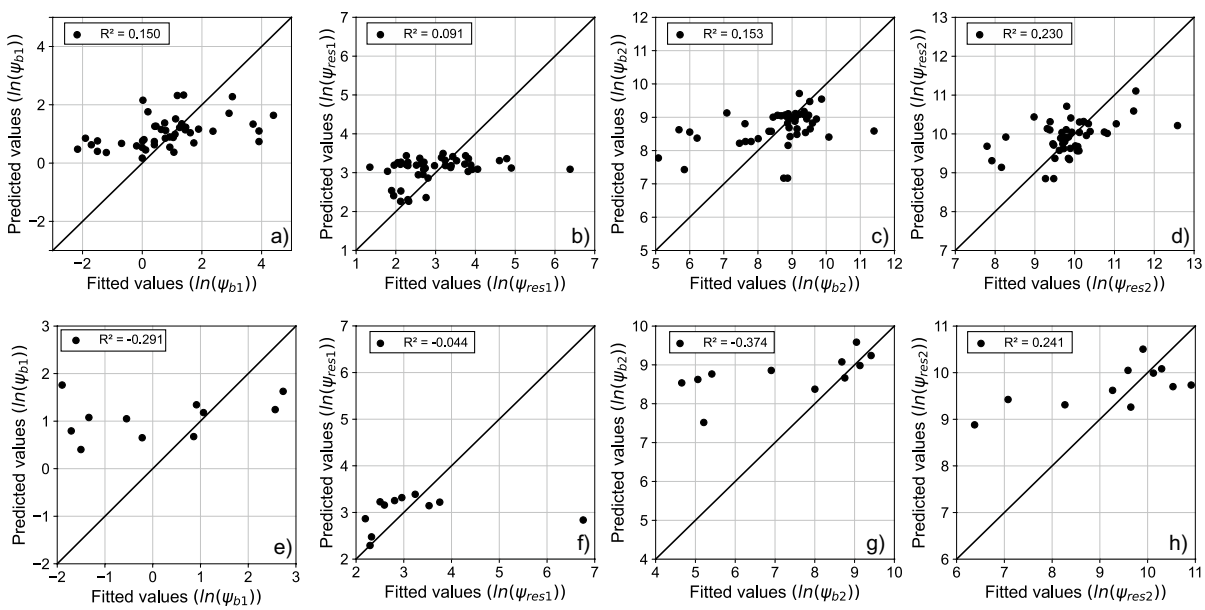

Fig. 6 Comparison of fitted and predicted values: **a** training data, ψ_{b1}; **b** training data, ψ_{res1}; **c** training data, ψ_{b2}; **d** training data, ψ_{res2}; **e** test data, ψ_{b1}; **f** test data, ψ_{res1}; **g** test data, ψ_{b2}; **h** test data, ψ_{res2}

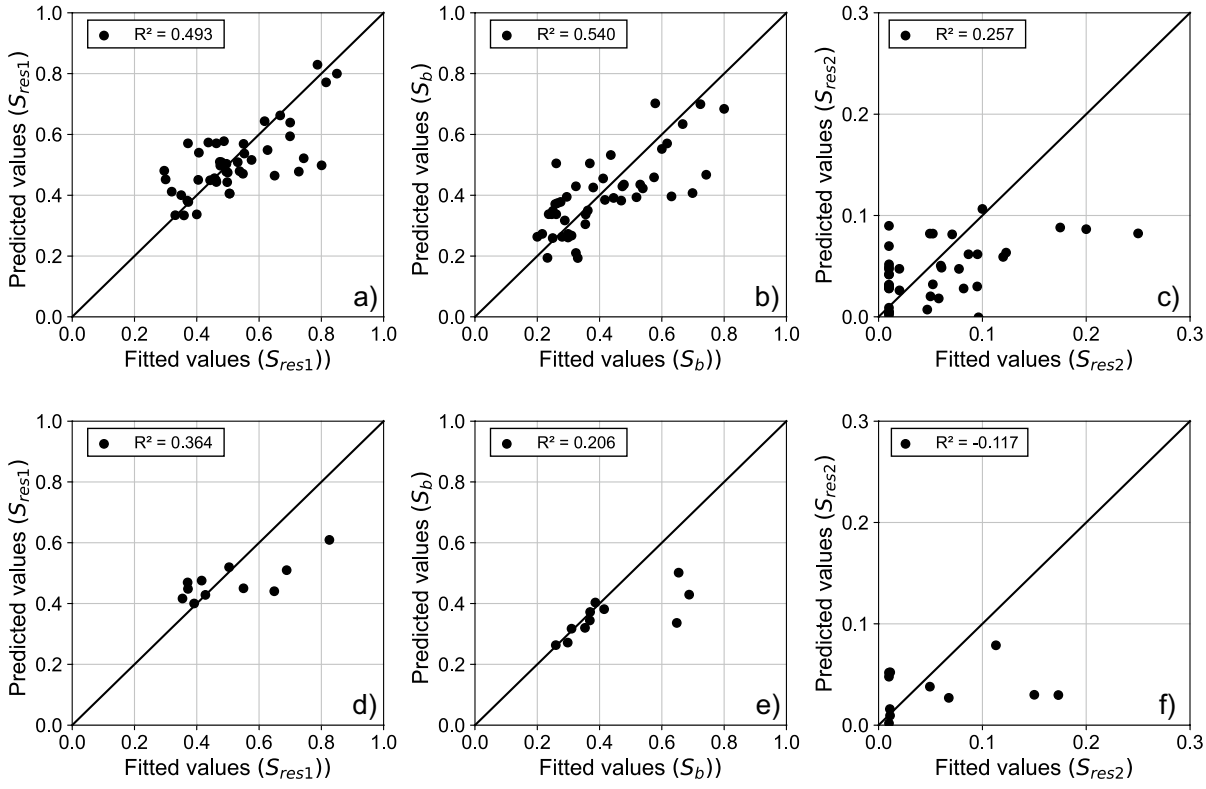

Fig. 8 Comparison of fitted and predicted values: **a** training data, S_{res1}; **b** training data, S_b; **c** training data, S_{res2}; **d** test data, S_{res1}; **e** test data, S_b; **f** test data, S_{res2}

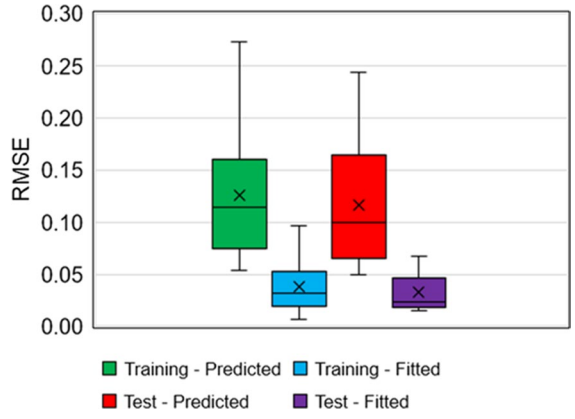

Fig. 9 Relative error and RSS predicted and fitted for training data and testing data

determination of GSDs in the two aggregation states is a standard procedure in the study of tropical soils as it provides information regarding the degree of weathering, stability of clay aggregates, among other data (Camapum de Carvalho and Gitirana Jr. 2021).

As presented in the previous section, 55 SWCC and 49 GSD datasets were collected from the literature. The collected information was randomly segregated, with 84% of the data being used from ANN training data and the remaining being utilized as test data. Furthermore, in each training epoch, the ANN considered a cross-validation, using 20% of the training data for this. The selected data was varied in each epoch and was totally randomized.

In addition to the parameters shown in Fig. 4, a bias was also used in each input layer. The bias is a unitary parameter used to allow the translation of the linear combination between the parameters of each layer and their respective weights, allowing flexibility to the network.

The parameters ψ_{b1}, ψ_{res1}, ψ_{b2}, and ψ_{res2} were predicted by the first ANN, as presented in Fig. 4. Two hidden layers were used, the first with six neurons and the second with eight neurons. The first layer used the

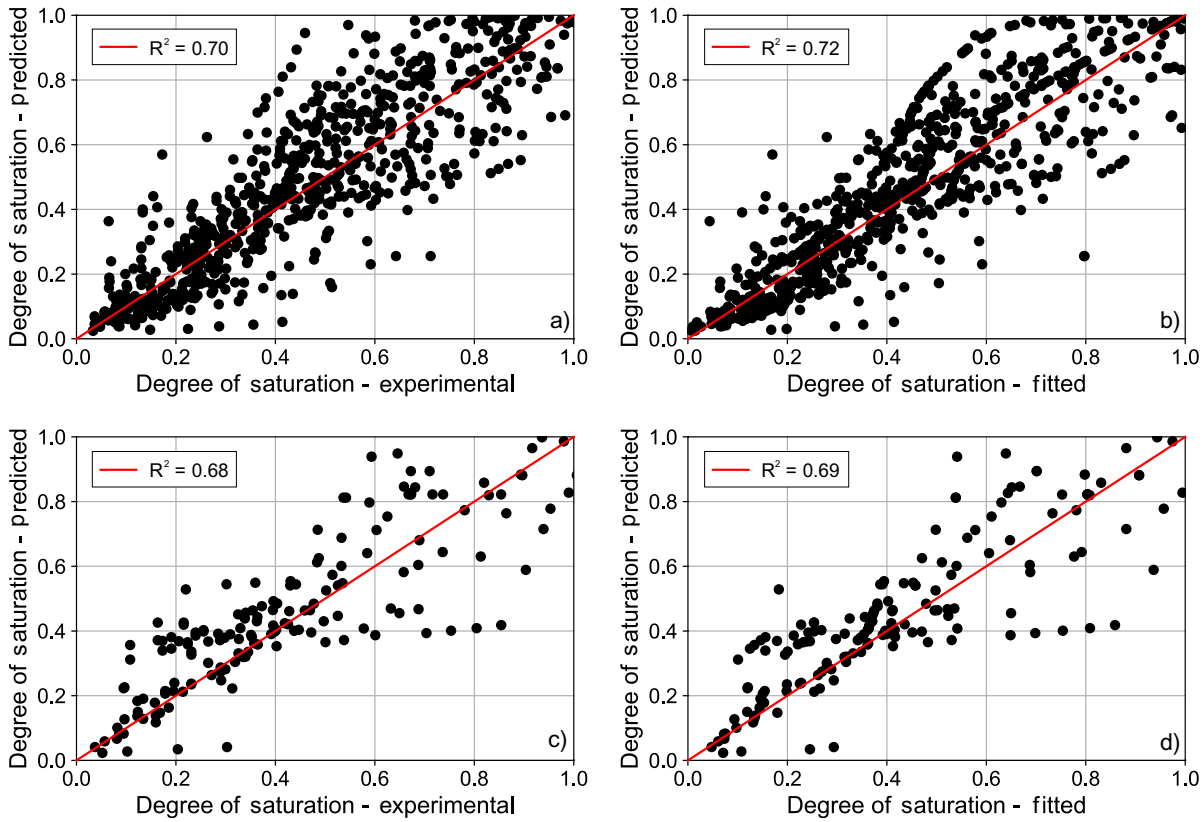

Fig. 10 Relationship between experimental, fitted, and predicted values: **a** experimental versus predicted (ANN training); **b** fitted versus predicted (ANN training); **c** experimental versus predicted (ANN test); **d** fitted versus predicted (ANN test)

hyperbolic tangent activation function, and the second layer used the ReLU function. The output function was the linear function. RMSprop was chosen as the optimizing method and the *MSE* (Mean Squared Error) was adopted as the loss function. For training the network 700 epochs were necessary, reaching a loss value $MSE = 0.059$.

The second ANN was designed for the prediction of the degree of saturation parameters S_{res1}, S_b and S_{res2}. This ANN comprises two hidden layers. The first hidden layer has six neurons and uses the hyperbolic tangent function. The second hidden layer has eight neurons and employs the ReLU activation function. The output function was linear. RMSProp was used as the optimizing method, while the *MSE* was adopted as the loss function. For training the network 700 epochs were necessary, reaching a loss value $MSE = 0.009$.

To analyze the training capability of the ANN presented in this paper, a comparison was performed with the models proposed by Arya and Paris (1981), Satyanaga et al. (2013), Zhang and Schaap (2017), called ROSETTA, and Rudiyanto et al. (2021), called NeuroFX. The models of Arya and Paris (1981), ROSETTA and Rudiyanto et al. (2021) were developed for unimodal soils. These models were selected to demonstrate the limitations of using prediction models that were not specially designed for bimodal soils. The model proposed by Satyanaga et al. (2013) was developed for bimodal soils but did not consider the special case of highly weathered tropical soils.

Due to its complex mathematical nature, ANN models are often deemed black boxes. As a result, it may be difficult to interpret the model behavior (Li and Vanapalli 2021). Nevertheless, sensitivity analyses can be performed to assess the impact of each input variable on the network output. A sensitivity analysis was therefore conducted using base value tornado diagrams. Gitirana Jr. (2005) and Franco et al. (2019) describe how these diagrams are established

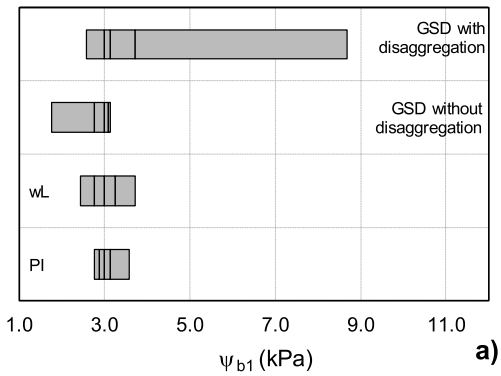
GSD with disaggregation
GSD without disaggregation
wL
PI
1.0
3.0
5.0
7.0
9.0
11.0
ψ b1 (kPa)
a)

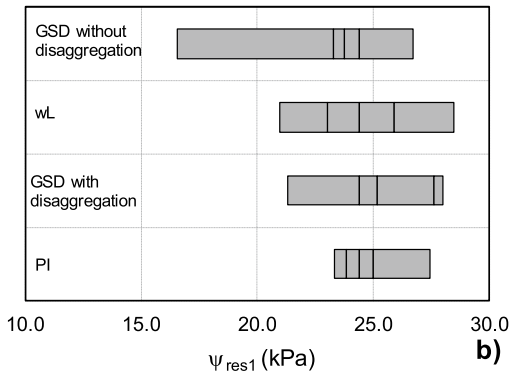
GSD without disaggregation
wL
GSD with disaggregation
PI
10.0
15.0
20.0
25.0
30.0
ψ res1 (kPa)
b)

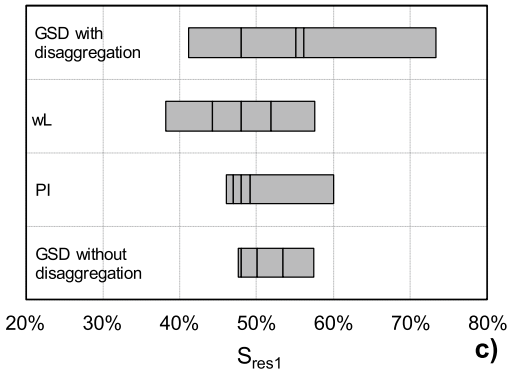
GSD with disaggregation
wL
PI
GSD without disaggregation
20%
30%
40%
50%
60%
70%
80%
S res1
c)

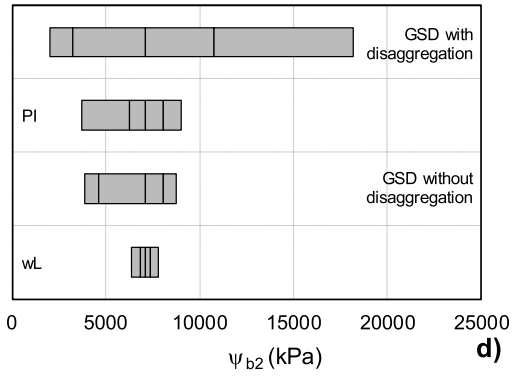
GSD with disaggregation
PI
GSD without disaggregation
wL
0
5000
10000
15000
20000
25000
ψ b2 (kPa)
d)

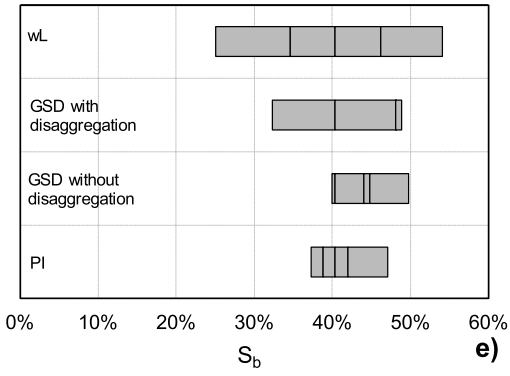
wL
GSD with disaggregation
GSD without disaggregation
PI
0%
10%
20%
30%
40%
50%
60%
S b
e)

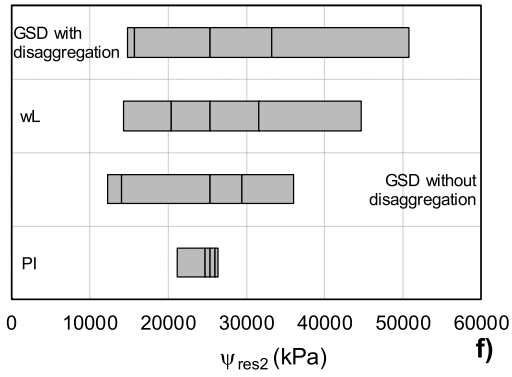
GSD with disaggregation
wL
GSD without disaggregation
PI
0
10000
20000
30000
40000
50000
60000
ψ res2 (kPa)
f)

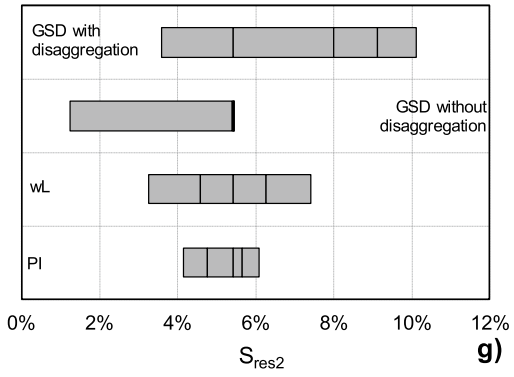
GSD with disaggregation
GSD without disaggregation
wL
PI
0%
2%
4%
6%
8%
10%
12%
S res2
g)

◂**Fig. 11** Tornado diagram for each coefficient of the bimodal equation of Gitirana Jr. and Fredlund (2004)

and interpreted. To construct the tornado diagram, the average, ± 1 standard deviation, maximum and minimum GSD scenarios were obtained, and diagrams were calculated for each input variable.

4 Results and Discussions

4.1 Prediction of Suction Parameters (ANN 1)

The parameters ψ_{b1}, ψ_{res1}, ψ_{b2}, and ψ_{res2} were predicted by the first ANN, as presented in Fig. 4. For training the network 700 epochs were necessary, reaching $MSE = 0.059$. Figure 5 shows the behavior of the *MSE* throughout the training process.

The trend of decreasing MSE value stabilized after 100 epochs. When the network stabilized after training, the MSE reached during validation was close to that obtained in training. The number of epochs was kept at 700 because some adjustments that improved the performance of the ANN were observed at later stages and did not cause overfitting. A total of 146 parameters were trained, 54 between the input and the first layer, 56 between the first layer and the second layer, and 36 between the third layer and the output.

Figure 6 shows the relationship between predicted and fitted values for ψ_{b1}, ψ_{res1}, ψ_{b2} and ψ_{res2}. There was better estimation during training compared to the ANN test. It is also possible to see that the network showed a relative ability to generalize the values, despite its poor performance. It is noteworthy that the ψ_{res2} parameter was the one that presented the best training and application in the test base, with R^2 greater than zero in both. Significant difficulty in prediction the air-entry and residual suction values of the macropores (i.e., ψ_{b1}, ψ_{res1}) is observed. This can be attributed to the higher variability of these parameters and more substantial complexity of the physical processes controlling the water retention in the macropores of bimodal soils (Camapum de Carvalho and Gitirana Jr. 2021).

Schaap and Bouten (1996) and Schaap et al. (2001) also showed that predicting the parameters analyzed in Fig. 6 can be challenging, due to the complex nature of the relationships between the SWCC and the other soil properties. For example, the model developed by Schaap et al. (2001) offered R^2 values ranging from 0.066 to 0.387. Another example is Rudiyanto et al. (2021), who found low R^2 values for the coefficients of the Fredlund and Xing (1994) equation, ranging from 0.072 to 0.355, and obtained good R^2 values, between 0.71 and 0.85 when evaluating the water retention data. It is important to note that these previous studies demonstrated that assessing the behavior of the model as a whole (i.e., not the individual parameters) provides a better picture of model performance. This type of evaluation will be presented later. It is also important to consider that bimodal soils have complex behavior due to their complex fabric, which should further increase modeling difficulties.

4.2 Prediction of Degree of Saturation Parameters (ANN 2)

The second ANN was designed for the prediction of the degree of saturation parameters S_{res1}, S_b and S_{res2}. For training the network, 700 epochs were necessary, reaching $MSE = 0.009$. Figure 7 shows the behavior of the *MSE* during training.

It is possible to see in Fig. 7 that the behavior of the MSE over the epochs was similar to that observed in ANN 1 (Fig. 6). After 100 epochs there is a tendency of stabilization of the MSE, approaching values below 0.009. ANN 2 was kept at 700 epochs for the same reason as ANN 1. A total of 137 parameters were trained, 54 between the input and first layer, 56 between the first and second layer, and 27 between the second layer and the output.

Figure 8 shows the relationship between predicted and fitted values for S_{res1}, S_b and S_{res2}. Figure 8 shows better training and generalization ability of the saturation degree parameters compared to the suction coefficients obtained using the ANN 1, but it is not yet possible to say that the R^2 achieved is good. S_{res2} showed an R^2 smaller than zero for the test, indicating some difficulty in ANN learning for this parameter. Again, the challenges reported by Schaap and Bouten (1996) and Schaap et al. (2001) apply to this situation. It is important to evaluate how the coefficients work together in predicting the SWCC, to confirm whether the model is suitable (Rudiyanto et al. 2021).

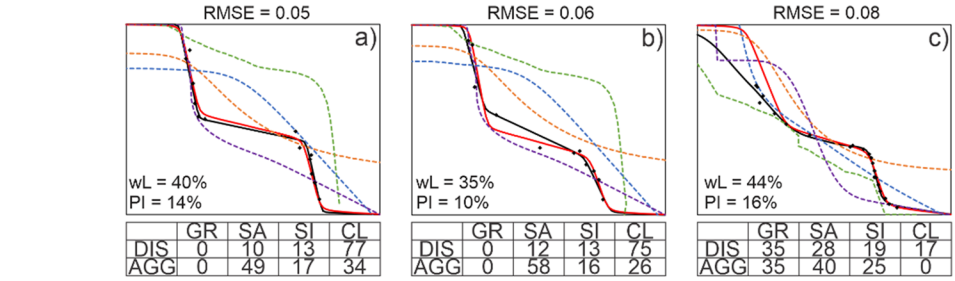

	GR	SA	SI	CL
DIS	0	10	13	77
AGG	0	49	17	34

	GR	SA	SI	CL
DIS	0	12	13	75
AGG	0	58	16	26

	GR	SA	SI	CL
DIS	35	28	19	17
AGG	35	40	25	0

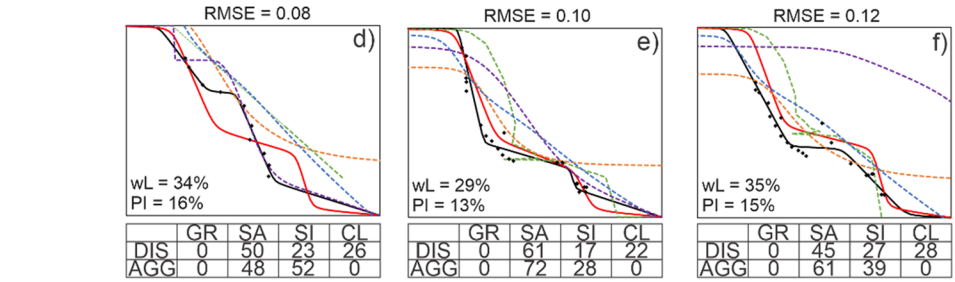

	GR	SA	SI	CL
DIS	0	50	23	26
AGG	0	48	52	0

	GR	SA	SI	CL
DIS	0	61	17	22
AGG	0	72	28	0

	GR	SA	SI	CL
DIS	0	45	27	28
AGG	0	61	39	0

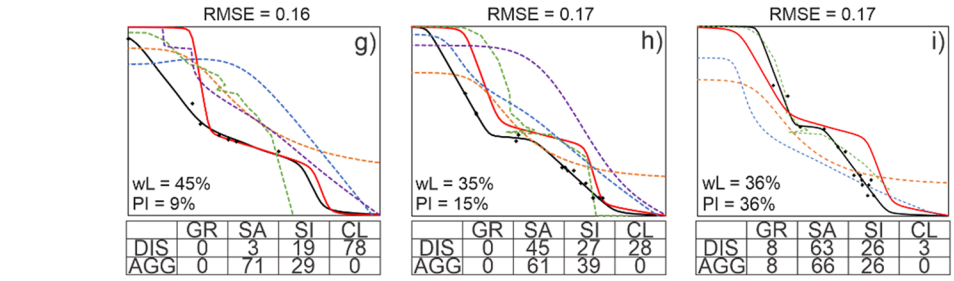

	GR	SA	SI	CL
DIS	0	3	19	78
AGG	0	71	29	0

	GR	SA	SI	CL
DIS	0	45	27	28
AGG	0	61	39	0

	GR	SA	SI	CL
DIS	8	63	26	3
AGG	8	66	26	0

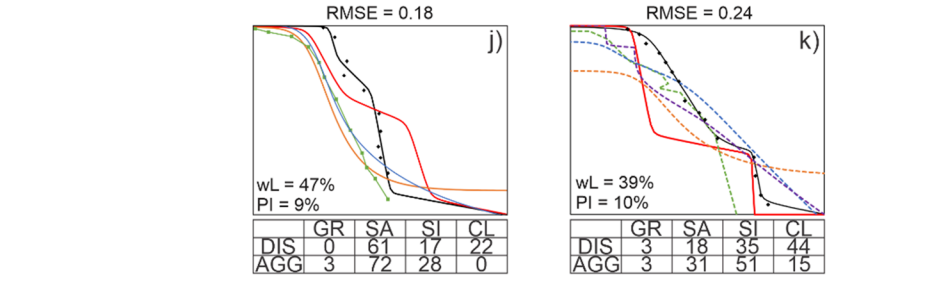

	GR	SA	SI	CL
DIS	0	61	17	22
AGG	3	72	28	0

	GR	SA	SI	CL
DIS	3	18	35	44
AGG	3	31	51	15

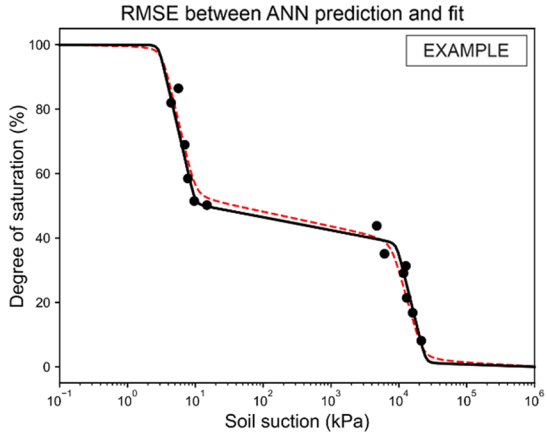

Caption

SWCC fitted from experimental data
SWCC fitted from grain-size distribution curve
Arya and Paris
Rosetta
Satyanaga et al.
NeuroFX

GR: Gravel
SA: Sand
SI: Silt
CL: Clay
DIS: with disaggregation
AGG: without disaggregation
The numbers are the percentages of each fraction

◂**Fig. 12** Panel of fitted and predicted curves, showing the GSD and the w_L and *PI* of each soil, for the bimodal curve

4.3 Bimodal SWCC Prediction

Figure 9 presents the distribution of the root mean squared error (RMSE) values, between the fitted and predicted degree of saturation data points, for the test and training databases. Overall, the average RMSE of the predicted values proved to be larger than the fitted one. However, this fact is expected since the ANN offers an approximate prediction while the fitted results indicate the capability of the fitting equation. Therefore, the RMSE values obtained using the fitting equation provide a reference value that could hardly be matched by estimation models.

Figure 10 presents the relationship between experimental, fitted, and predicted values of degree of saturation. Values of R^2 higher than 0.68 were observed for the test and training datasets, corroborating the low RMSE values presented in Fig. 9. This result is in line with the values provided by other ANNs in the same category, as presented in Table 1. Similar R^2 values are found when comparing the experimental and predicted values (Fig. 10a, c) with the fitted and predicted values (Fig. 10b, d). These results indicate that the best-fit procedure adopted to obtain the parameters of the Gitirana Jr. and Fredlund (2004) equation were adequate and close to the experimental values, in agreement with the low RMSE values presented in Fig. 9.

4.4 Sensitivity Analysis

Figure 11 shows the tornado diagrams obtained. In general, the output variables tend to be very sensitive to the input variables, but some input variables are more important than others. It is also interesting to note that the relationships between input and output variables tend to reflect features of soil behavior that are meaningful.

GSD with disaggregation is the variable with the greatest impact on the network. The high influence of grain-size distribution was expected, since the proportion of each textural class dictates the shape of the SWCC, as well as being directly related to the pore-size distribution. The parameter ψ_{res2} is mostly dependent on w_L. The variable *PI* had the greatest influence on ψ_{b2}, for the same reasons. In the residual zones and in the micropore region, the influence of w_L and *PI* can be seen, which is directly related to the water retention capacity of fine particle (Aubertin et al. 2003).

4.5 Comparison with Other Models

Figure 12 presents examples of prediction exercises for soils of the test base. Comparisons are presented for the SWCC obtained using the best-fit nonlinear regression analysis, the prediction ANN proposed herein and four prediction models from the literature. Firstly, regarding the prediction performed by the developed ANN, it is possible to note good fitting capabilities, as already evidenced in Figs. 9 and 10. It can be observed that even without the imposition of restriction conditions in the ANN, the curve format adequately followed the bimodal shape and overall water retention characteristics.

Despite its generally adequate fit, the model has some limitations. For example, the model has difficulty predicting the air-entry value, especially for lower values, as seen in Fig. 12c, g, h, but also for slightly higher values, as seen in Fig. 12i, j. This behavior was expected given the results obtained in Fig. 6e. The ANN model also presented difficulty in dealing with smaller distances between the first residual point and the second air-entry value, as can be seen in Fig. 12d, i, j. These limitations resulted in relatively lower performance in some cases, as seen in Fig. 12d, j, k.

The example shown in Fig. 12i is a tropical bimodal soil with a very low level of particle aggregation. As can be seen in Fig. 12i, only 3% of the clay was aggregated. Another point is that it was not possible to measure the plasticity limit of the soil. A *PI* equal to *wL* was considered for the calculation. Even in this atypical scenario, the model was able to make a good prediction for the macropore region, but there were difficulties in the micropore region, mainly due to the difficulty of the mesh to handle short distances between the first residual point and the second air entry point.

Furthermore, it is possible to perceive the poor performance of the previous models, selected from the literature. It should be noted that the models of Arya and Paris (1981), ROSETTA, and NeuroFX were developed for unimodal soils and are presented

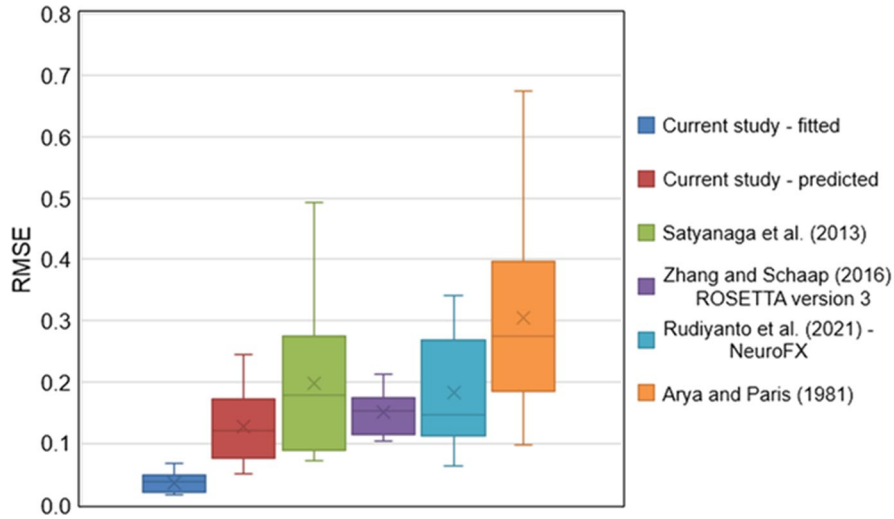

Fig. 13 Distribution of RMSE values for each model applied to the test-base soils

here just as a base for comparison. However, these three models can still offer prediction with moderate performance in the macropore region of the SWCC. The Arya and Paris (1981) model even has a good prediction over most of the SWCC in Fig. 12i. The model proposed by Satyanaga et al. (2013) for bimodal soils was also applied to the test data, even though this model was also not specifically designed for tropical soils. It is possible to perceive poor prediction results, with some curves not presenting the bimodal shape. This result for the Satyanaga et al. (2013) model is consistent with the findings of Neves et al. (2022).

Figure 13 presents the distribution of the residual mean squared error (RMSE) values for each of the predicted curves presented in Fig. 12. The ANN showed better RMSE values when compared to the other four prediction models. Among the four models selected from the literature, the one that presented the best performance was ROSETTA. This is due to the good fit in the macro-pore region, as can be seen in Fig. 12. Although the Satyanaga et al. (2013) model presented a bimodal format in most cases, it showed high RMSE values with poor predictions for the nine testing soils (Fig. 12). It is important to note, however, that the Satyanaga et al. (2013) model was not intended for and did not consider the special features of tropical soils. In summary, the comparisons presented herein indicate that the four selected estimation models should not be applied to tropical bimodal soils.

5 Conclusions

An artificial neural network prediction model for the soil–water characteristic curve (SWCC) of bimodal tropical soils was presented. The model is based on the grain-size distribution (GSD) and on the liquid limit, and plasticity index. Information regarding the degree of particle aggregation was included in the form of GSDs for the soil in the aggregated and disaggregated conditions. The model showed adequate prediction capabilities, with R^2 values of 0.72 for the training data and of 0.69 for the test data. Even though the individual parameters had R^2s less than 0.69, with some even negative, the final response of the model was satisfactory. This phenomenon was present in other models in the literature, such as Schaap and Bouten (1996), Schaap et al. (2001) and Rudiyanto et al. (2021), and its answer lies in the fact that the equation works on the coefficients together to arrive at the final water retention value, even in a situation where the coefficients are well-defined points of the SWCC, as is the case with the equation of Gitirana Jr. and Fredlund (2004).

The proposed model introduces the use of ANN for the prediction of bimodal soils and shows great potential for application to the bimodal soils. Although this study utilized data from a specific Brazilian region, all the methodology developed here can easily be applied to other types of soils in various regions of the world, as in Schaap et al. (2001), Minasny and McBratney (2002) and Haghverdi et al.

(2012). Similar performance of the current ANN model for tropical bimodal soils from other regions of the world cannot be guaranteed and future tests are necessary.

Several future improvements can be implemented to the developed ANN, such as the incorporation of parameters related to soil porosity, which is directly related to soil suction. The availability of complete datasets of soil testing data is a major obstacle to the construction of ANN models. In machine learning methods, larger quantities of data generally lead to more accurate training. The creation of larger soils databases of bimodal tropical soils will allow the exploration of machine learning tools in the understanding of tropical soils behavior.

Trial and error are an important aspect of the methodology of developing ANNs. Therefore, it is not possible to state that the proposed architecture could not be further improved, as larger datasets become available. Other activation and output functions, variations in the number of layers and neurons, as well as other forms of data standardization could be explored in the future.

The modeling decision to adopt degree of saturation was likely key to the successful development of the ANN. In terms of practical application of the ANN, the SWCCs predicted in terms of degree of saturation can be combined with directly determined porosity and compressibility information to convert the SWCC to gravimetric or volumetric water content. It is important to note, however, that the air-entry values, residual conditions, and partitioning between micro and microporosity are also dependent on natural and compaction conditions, even though to a lesser degree when compared to porosity (Rahardjo et al. 2012). In this sense, it is valuable to consider that these modeling decisions may result in limitations of the ANN.

Acknowledgements The authors are thankful for the financial support provided by FAPEG (*Fundação de Amparo à Pesquisa do Estado de Goiás*, in English: Goias State Research Support Foundation).

Data availability The datasets generated during and/or analyzed during the current study are available from the corresponding author upon reasonable request.

Declarations

Conflict of interest The authors declare that they have no conflict of interest.

References

ABNT—Associação Brasileira de Normas Técnicas (2016) NBR 6459—soil—determination of the liquid limit. Rio de Janeiro (in Portuguese)

ABNT—Associação Brasileira de Normas Técnicas (2016) NBR 7180—soil—determination of the plastic limit. Rio de Janeiro (in Portuguese).

Achieng KO (2019) Modelling of soil moisture retention curve using machine learning techniques: artificial and deep neural networks vs support vector regression models. Comput Geosci 133:104320. https://doi.org/10.1016/j.cageo.2019.104320

Aguiar LA (2010) Contributions to the analysis of the mechanical behavior of compacted soils for use in dams. Dissertation, Universidade de Brasilia (in Portuguese)

Aguiar LA (2014) Analysis of the mechanical behavior of compacted and chemically stabilized soils for use in dams. Thesis, Universidade de Brasilia (in Portuguese)

Albuquerque EAC, Borges LPF, Cavalcante ALB, Machado SB (2022) Prediction of soil water retention curve based on physical characterization parameters using machine learning. Soils Rocks. https://doi.org/10.28927/SR.2022.000222

Almeida JGR, Romão PA, Mascarenha MMA, Sales MM (2015) Erodibility of unsaturated tropical soils in the municipalities of Senador Canedo and Bonfinópolis (GO). Revista Geociências 34(3):441–451 (**in Portuguese**)

Alves RD, Gitirana GFN Jr, Vanapalli SK (2020) Advances in the modeling of the soil–water characteristic curve using pore-scale analysis. Comput Geotech 127:103766. https://doi.org/10.1016/j.compgeo.2020.103766

Amadi AA, Osinubi KJ, Okoro JI (2023) Hydraulic conductivity of unsaturated specimens of lateritic soil-bentonite mixtures. Geotech Geol Eng. https://doi.org/10.1007/s10706-023-02524-3

Amanabadi S, Vazirinia M, Vereecken H, Vakilian KA, Mohammadi MH (2019) Comparative study of statistical, numerical and machine learning-based pedotransfer functions of water retention curve with particle size distribution data. Eurasian Soil Sci 52:1555–1571. https://doi.org/10.1134/S106422931930001X

Angelim RR, Cunha RP, Sales MM (2016) Determining the elastic deformation modulus from a compacted earth embankment via laboratory and Ménard pressuremeter tests. Soils Rocks 39(3):285–300. https://doi.org/10.28927/SR.393285

Araujo AG (2010) Performance analysis of infiltration wells in the city of Goiânia-GO. Dissertation, Universidade Federal de Goiás (**in Portuguese**)

Araujo AG, Souza JC, Alves EC, Silva IL, Correchel V (2017) Application of models of adjustments of soil water characteristics curves in tropical soils. Revista Mirante 10(5a) (**in Portuguese**)

Arya LM, Paris JF (1981) A physicoempirical model to predict soil moisture characteristics from particle-size distribution and bulk density data. Soil Sci Soc Am J 45:1023–1030. https://doi.org/10.2136/sssaj1981.03615995004500060004x

Aubertin M, Mbonimpa M, Bussière B, Chapuis RP (2003) A model to predict the water retention curve from basic geotechnical properties. Can Geotech J 40(6):1104–1122. https://doi.org/10.1139/t03-054

Ayala RJL (2020) Soil improvement with fibers from the poultry industry. Thesis, Universidade de Brasilia (**in Portuguese**)

Bayat H, Neyshaburi MR, Mahammadi K, Nariman-Zadeh N, Irannejad M, Gregory AS (2013) Combination of artificial neural networks and fractal theory to predict soil water retention curve. Comput Electron Agric 92:92–103. https://doi.org/10.1016/j.compag.2013.01.005

Bayat H, Mazaheri B, Mohanty BP (2019) Estimating soil water characteristic curve using landscape features and soil thermal properties. Soil Tillage Res 189:1–14. https://doi.org/10.1016/j.still.2018.12.018

Belik AA, Bolotov AG, Shein EV, Kokoreva AA, Levin AA, Patrushev VY (2019) Application of neural network pedotransfer functions to calculate soil water retention curve. In: IOP conference series: earth and environmental science. IOP Publishing, p 012008

Borges CR (2014) Microstructural study of the hydromechanical behavior of the soil of Brasília-DF. Thesis, Universidade de Brasilia (**in Portuguese**)

Campos-Guereta I, Dawson A, Thom N (2021) An alternative continuous form of Arya and Paris model to predict the soil water retention curve of a soil. Adv Water Resour 154:103968. https://doi.org/10.1016/j.advwatres.2021.103968

Carducci CE, Oliveira GC, Severiano EC, Zeviani WM (2011) Modeling the water retention curve in Oxisols using the Double Van Genuchten Equation. Revista Brasileira de Ciência do Solo 35(1):77–86. https://doi.org/10.1590/S0100-06832011000100007. (**in Portuguese**)

Camapum de Carvalho J, Gitirana GFN Jr (2021) Unsaturated soils in the context of tropical soils. Soils Rocks. https://doi.org/10.28927/SR.2021.068121

Carvalho RB (2014) Geotechnical evaluation of stormwater infiltration wells. Universidade de Brasilia (in Portuguese), Thesis

D'Emilio A, Aiello R, Consoli S, Vanella D, Iovino M (2018) Artificial neural networks for predicting the water retention curve of sicilian agricultural soils. Water 10(10):1431. https://doi.org/10.3390/w10101431

Dias MCC (2014) Feasibility of using tropical soil and construction waste in landfill cover systems. Dissertation, Universidade Federal de Goiás (**in Portuguese**)

Diemer F (2014) Characterization of the strength of a tropical soil from the dynamic cone penetration test with variable energy (PANDA). Dissertation, Universidade Federal de Goiás (**in Portuguese**)

Ebrahimi E, Bayat H, Neyshaburi MR, Abyaneh HZ (2014) Prediction capability of different soil water retention curve models using artificial neural networks. Arch Agron Soil Sci 60(6):859–879. https://doi.org/10.1080/03650340.2013.837219

Falcão PR, Baroni M, Masutti GC, Pinheiro RJB, Fagundes DF (2023) Assessment of the impact of inundation on the strength of a lateritic and collapsible soil. Geotech Geol Eng 41(8):4761–4773. https://doi.org/10.1007/s10706-023-02545-y

Farias WM (2012) Evolutionary processes of chemical weathering and their action on the hydromechanical behavior of soils from the central plateau. Thesis, Universidade de Brasilia (**in Portuguese**)

Foko Tamba C, Kengni L, Tematio P, Manefouet BI, Kenfack JV (2022) Assessment of lateritic gravelled materials for use in road pavements in Cameroon. Geotech Geol Eng 40(8):4195–4215. https://doi.org/10.1007/s10706-022-02151-4

Franco VH, Gitirana GFN Jr, Assis AP (2019) Probabilistic assessment of tunneling-induced building damage. Comput Geotech 113:103097. https://doi.org/10.1016/j.compgeo.2019.103097

Fredlund DG (2000) The 1999 RM Hardy Lecture: The implementation of unsaturated soil mechanics into geotechnical engineering. Can Geotech J 37(5):963–986. https://doi.org/10.1139/t00-026

Fredlund DG, Xing A (1994) Equations for the soil-water characteristic curve. Can Geotech J 31(4):521–532. https://doi.org/10.1139/t94-061

Fredlund DG, Xing A, Huang S (1994) Predicting the permeability function for unsaturated soils using the soil–water characteristic curve. Can Geotech J 31(4):533–546. https://doi.org/10.1139/t94-062

Fredlund DG, Xing A, Fredlund MD, Barbour SL (1996) The relationship of the unsaturated soil shear strength to the soil–water characteristic curve. Can Geotech J 33(3):440–448. https://doi.org/10.1139/t96-065

Fredlund DG, Rahardjo H, Fredlund MD (2012) Unsaturated soil mechanics in engineering practice. John Wiley & Sons Inc

Freitas JB, Rezende LR, Gitirana GFN Jr (2020) Prediction of the resilient modulus of two tropical subgrade soils considering unsaturated conditions. Eng Geol 270:105580. https://doi.org/10.1016/j.enggeo.2020.105580

Garg A, Wani I, Zhu H, Kushvaha V (2022) Exploring efficiency of biochar in enhancing water retention in soils with varying grain size distributions using ANN technique. Acta Geotech 17:1315–1326. https://doi.org/10.1007/s11440-021-01411-6

Gitirana Jr GFN (2005) Weather-related geo-hazard assessment model for railway embankment stability. Thesis, University of Saskatchewan

Gitirana GFN Jr, Fredlund DG (2004) Soil–water characteristic curve equation with independent properties. J Geotech Geoenviron Eng 130(2):209–212. https://doi.org/10.1061/(ASCE)1090-0241(2004)130:2(209)

Gitirana GFN Jr, Fredlund DG (2016) Statistical assessment of hydraulic properties of unsaturated soils. Soils Rocks 39(1):81–95. https://doi.org/10.28927/SR.391081

Grau EDA (2014) Effect of moisture variation on thrust in tropical soils. Dissertation, Universidade de Brasilia (**in Portuguese**).

Gomes AC (2015) Monitoring of a spaced pile retaining wall considering suction profile. Dissertation, Universidade Federal de Goiás (**in Portuguese**).

Haghverdi A, Cornelis WM, Ghahraman B (2012) A pseudo-continuous neural network approach for developing water retention pedotransfer functions with limited data. J Hydrol 442:46–54. https://doi.org/10.1016/j.jhydrol.2012.03.036

Haghverdi A, Öztürk HS, Durner W (2018) Measurement and estimation of the soil water retention curve using the evaporation method and the pseudo continuous pedotransfer function. J Hydrol 563:251–259. https://doi.org/10.1016/j.jhydrol.2018.06.007

Haykin S (1999) Neural networks: a comprehensive foundation. Delhi, India

Jain SK, Singh VP, van Genuchten MT (2004) Analysis of soil water retention data using artificial neural networks. J Hydrol Eng 9(5):415–420. https://doi.org/10.1061/(ASCE)1084-0699(2004)9:5(415)

Javanshir S, Bayat H, Gregory AS (2020) Effect of free swelling index on improving estimation of the soil moisture retention curve by different methods. CATENA 189:104479. https://doi.org/10.1016/j.catena.2020.104479

Jesus AC (2013) Multidisciplinary investigation of linear erosive processes: a case study of the city of Anápolis-GO. Universidade de Brasilia (in Portuguese), Thesis

KERAS (2022) Keras. https://keras.io/. Acessed 13 March 2022

Koekkoek EJW, Booltink H (1999) Neural network models to predict soil water retention. Eur J Soil Sci 50(3):489–495. https://doi.org/10.1046/j.1365-2389.1999.00247.x

Leong EC, He L, Rahardjo H (2002) Factors affecting the filter paper method for total and matric suction measurements. Geotech Test J 25(3):322–333. https://doi.org/10.1520/GTJ11094J

Li Y, Vanapalli SK (2021) Prediction of soil-water characteristic curves using two artificial intelligence (AI) models and AI aid design method for sands. Can Geotech J 59(1):129–143. https://doi.org/10.1139/cgj-2020-0562

Lopera JFB (2016) Influence of microstructure on the mechanical behavior of natural and compacted tropical soils. Dissertation, Universidade de Brasilia (**in Portuguese**)

Luiz GC (2012) Influence of the soil-atmosphere relationship on the hydromechanical behavior of unsaturated tropical soils: case study—municipality of Goiânia-GO. Thesis, Universidade de Brasilia (**in Portuguese**)

Matos THC (2011) Hydro-mechanical characterization of phosphogypsum and soil-phosphogypsum mixtures. Dissertation, Universidade de Brasilia (**in Portuguese**)

Melo TM, Pedrollo OC (2015) Artificial neural networks for estimating soil water retention curve using fitted and measured data. Appl Environ Soil Sci. https://doi.org/10.1155/2015/535216

Mendes TA, Pereira SAS, Souza WAR, Rebolledo JFR, Gitirana GFN Jr, Sales MM, Luz MP (2022) Physical and numerical modelling of infiltration and runoff in unsaturated exposed soil using a rainfall simulator. Soil Res 61(3):267–283. https://doi.org/10.1071/SR22181

Miguel MG, Bonder BH (2012) Soil–water characteristic curves obtained for a colluvial and lateritic soil profile considering the macro and micro porosity. Geotech Geol Eng 30:1405–1420. https://doi.org/10.1007/s10706-012-9545-y

Minasny B, McBratney AB (2002) The neuro-m method for fitting neural network parametric pedotransfer functions. Soil Sci Soc Am J 66(2):352–361. https://doi.org/10.2136/sssaj2002.3520

Minasny B, Mcbratney AB, Bristow KL (1999) Comparison of different approaches to the development of pedotransfer functions for water-retention curves. Geoderma 93(3–4):225–253. https://doi.org/10.1016/S0016-7061(99)00061-0

Neves JP, Alves RD, Gitirana Jr. GFN, Mendes TA (2022) Application of a soil-water characteristic curve prediction model to bimodal tropical soils. In: XX Congresso Brasileiro de Mecânica dos Solos e Engenharia Geotécnica, Campinas, Brazil (**in Portuguese**)

Ng CW, Pang YW (2000) Influence of stress state on soil-water characteristics and slope stability. J Geotech Geoenviron Eng 126(2):157–166. https://doi.org/10.1061/(ASCE)1090-0241(2000)126:2(157)

Ottoni MV, Ottoni Filho TB, Schaap MG, Lopes-Assad MLRC, Rotunno Filho OC (2018) Hydrophysical database for Brazilian soils (HYBRAS) and pedotransfer functions for water retention. Vadose Zone J 17(1):1–17. https://doi.org/10.2136/vzj2017.05.0095

Pachepsky YA, Timlin D, Varallyay GY (1996) Artificial neural networks to estimate soil water retention from easily measurable data. Soil Sci Soc Am J 60(3):727–733. https://doi.org/10.2136/sssaj1996.03615995006000030007x

Pham K, Kim D, Yoon Y, Choi H (2019) Analysis of neural network based pedotransfer function for predicting soil water characteristic curve. Geoderma 351:92–102. https://doi.org/10.1016/j.geoderma.2019.05.013

Pham TA, Sutman M, Medero GM (2023) Validation, reliability, and performance of shear strength models for unsaturated soils. Geotech Geol Eng 41(7):4271–4309. https://doi.org/10.1007/s10706-023-02520-7

Queiroz ACG (2015) Study of the microstructural behavior of compacted tropical soils. Thesis, Universidade de Brasilia (**in Portuguese**)

Qian J, Lin Z, Shi Z (2022) Experimental and modeling study of water-retention behavior of fine-grained soils with dual-porosity structures. Acta Geotech 17(8):3245–3258. https://doi.org/10.1007/s11440-022-01483-y

Rahardjo H, Satyanaga A, D'Amore GAR, Leong EC (2012) Soil–water characteristic curves of gap-graded soils. Eng Geol 125:102–107. https://doi.org/10.1016/j.enggeo.2011.11.009

Rastgou M, Bayat H, Gregory MMAS (2022) Estimating soil water retention curve by extreme learning machine, radial basis function, M5 tree and modified group method of data handling approaches. Water Resour Res. https://doi.org/10.1029/2021WR031059

Rudiyanto MB, Chaney NW, Maggi F, Giap SGE, Shah RM, Fiantis D, Setiawan BI (2021) Pedotransfer functions for estimating soil hydraulic properties from saturation to dryness. Geoderma 403:115194. https://doi.org/10.1016/j.geoderma.2021.115194

Saha S, Gu F, Luo X, Lytton RL (2018) Prediction of soil-water characteristic curve for unbound material using Fredlund–Xing equation-based ANN approach. J Mater

Civ Eng 30(5):06018002. https://doi.org/10.1061/(ASCE)MT.1943-5533.0002241

Satyanaga A, Rahardjo H, Leong EC, Wang JY (2013) Water characteristic curve of soil with bimodal grain-size distribution. Comput Geotech 48:51–61. https://doi.org/10.1016/j.compgeo.2012.09.008

Satyanaga A, Rahardjo H, Zhai Q, Moon S-W, Kim J (2023) Modelling particle-size distribution and estimation of soil–water characteristic curve utilizing modified lognormal distribution function. Geotech Geol Eng. https://doi.org/10.1007/s10706-023-02638-8

Schaap MG, Bouten W (1996) Modeling water retention curves of sandy soils using neural networks. Water Resour Res 32(10):3033–3040. https://doi.org/10.1029/96WR02278

Schaap MG, Leij FJ (1998) Using neural networks to predict soil water retention and soil hydraulic conductivity. Soil Tillage Res 47(1–2):37–42. https://doi.org/10.1016/S0167-1987(98)00070-1

Schaap MG, Leij FJ, van Genuchten MT (2001) Rosetta: a computer program for estimating soil hydraulic parameters with hierarchical pedotransfer functions. J Hydrol 251(3–4):163–176. https://doi.org/10.1016/S0022-1694(01)00466-8

Skalová J, Čistý M, Bezák J (2011) Comparison of three regression models for determining water retention curves. J Hydrol Hydromech 59(4):275–284. https://doi.org/10.2478/v10098-011-0023-7

Sillers WS, Fredlund DG, Zakerzadeh N (2001) Mathematical attributes of some soil–water characteristic curve models. Geotech Geol Eng. https://doi.org/10.1023/A:1013109728218

Silva MTMG (2009) Methodology for determining parameters for unsaturated soils using tests with known moisture. Dissertation, Universidade de Brasilia (**in Portuguese**)

Silva AP, Tormena CA, Fidalski J, Imhoff S (2008) Funções de pedotransferência para as curvas de retenção de água e de resistência do solo à penetração. Rev Bras Ciênc Solo 32(1):1–10. https://doi.org/10.1590/S0103-84782007000500015

Silva AC, Armindo RA, Prevedello CL (2020) Splintex 2.0: a physically-based model to estimate water retention and hydraulic conductivity parameters from soil physical data. Comput Electron Agric 169:105157. https://doi.org/10.1016/j.compag.2019.105157

Sobotkova M, Snehota M, Dohnal M, Ray C (2011) Determination of hydraulic properties of a tropical soil of Hawaii using column experiments and inverse modeling. Rev Bras Ciênc Solo 35(4):1229–1239. https://doi.org/10.1590/S0100-06832011000400016

Souza WAR, Pereira SAS, Mendes TA, Costa RF, Gitirana GFN Jr, Rebolledo JF (2022) Statistical evaluation of testing conditions on the saturated hydraulic conductivity of Brazilian lateritic soils using artificial intelligence approaches. Sci Rep 12:20381. https://doi.org/10.1038/s41598-022-24779-1

Tomasella J, Hodnett MG (1998) Estimating soil water retention characteristics from limited data in Brazilian Amazonia. Soil Sci 163(3):190–202. https://doi.org/10.1097/00010694-199803000-00003

Tomasella J, Hodnett MG, Rossato L (2000) Pedotransfer functions for the estimation of soil water retention in Brazilian soils. Soil Sci Soc Am J 64(1):327–338. https://doi.org/10.2136/sssaj2000.641327x

van Genuchten MT (1980) A closed-form equation for predicting the hydraulic conductivity of unsaturated soils. Soil Sci Soc Am J 44(5):892–898. https://doi.org/10.2136/sssaj1980.03615995004400050002x

Vanapalli SK, Fredlund DG, Pufahl DE, Clifton AW (1996) Model for the prediction of shear strength with respect to soil suction. Can Geotech J 33(3):379–392. https://doi.org/10.1139/t96-060

Wanderley Neto RV (2020) Experimental study of soil-concrete interfaces in the context of unsaturated soils. Dissertation, Universidade de Brasilia (**in Portuguese**)

Xu X, Li H, Sun C, Ramos TB, Darouich H, Xiong Y, Qu Z, Huang G (2021) Pedotransfer functions for estimating soil water retention properties of northern China agricultural soils: development and needs. Irrig Drain 70(4):593–608. https://doi.org/10.1002/ird.2584

Yan W, Birle E, Cudmani R (2021) A new framework to determine general multimodal soil water characteristic curves. Acta Geotech 16(10):3187–3208. https://doi.org/10.1007/s11440-021-01245-2

Zhai Q, Rahardjo H, Satyanaga A, Dai G (2020) Estimation of tensile strength of sandy soil from soil–water characteristic curve. Acta Geotech 15:3371–3381. https://doi.org/10.1007/s11440-020-01013-8

Zhai Q, Zhu Y, Rahardjo H, Satyanaga A, Dai G, Gong W, Zhao X, Ou Y (2023) Prediction of the soil–water characteristic curves for the fine-grained soils with different initial void ratios. Acta Geotechnica. https://doi.org/10.1007/s11440-023-01833-4

Zhao Y, Rahardjo H, Satyanaga A, Zhai Q, He J (2023) A general best-fitting equation for the multimodal soil–water characteristic curve. Geotech Geol Eng. https://doi.org/10.1007/s10706-023-02447-z

Zhang Y, Schaap MG (2017) Weighted recalibration of the Rosetta pedotransfer model with improved estimates of hydraulic parameter distributions and summary statistics (Rosetta3). J Hydrol 547:39–53. https://doi.org/10.1016/j.jhydrol.2017.01.004

Zhou AN, Sheng D, Carter JP (2012) Modelling the effect of initial density on soil-water characteristic curves. Géotechnique 62(8):669–680. https://doi.org/10.1680/geot.10.P.120